Scientia Iranica D (2015) 22(6), 2492–2504

Sharif University of Technology
Scientia Iranica
Transactions D: Computer Science & Engineering and Electrical Engineering
www.scientiairanica.com

A cellular automaton based model for visual perception based on anatomical connections

M. Beigzadeh and S.M.R. Hashemi Golpayegani*

Complex Systems and Cybernetic Control Lab, Faculty of Biomedical Engineering, Amirkabir University of Technology, 424 Hafez Ave, Tehran, P.O. Box 15875-4413, Iran.

Received 15 November 2014; received in revised form 29 June 2015; accepted 28 July 2015

KEYWORDS
Cellular automata;
Visual perception;
Coupled logistic maps;
Netlets;
Brain networks connections.

Abstract. A phenomenological model of visual perceptual dynamics is proposed based upon the Cellular Automata (CA) which considers the anatomical connections between visual areas of the macaque brain. Some other important characteristics of neural networks of the brain are also included in the model, such as the excitatory-inhibitory ratio of neural populations, synaptic delays, etc. A new form of "geometric mean interaction rules" among neural populations is also introduced which could be considered more realistic than current "arithmetic mean-based rules". This computational model is capable of showing interesting dynamical behaviors, seen in the visual perceptual states of the brain.

1. Introduction

The exploration to understand and somehow control biological systems, using fundamentals from physics and mathematics, has a long history [1]. Among biological systems, the mammalian brain, because of its vastly complex structure and its perfect and stable function, has attracted a special attention. Researchers try to mainly understand and mimic some behavioral and dynamical aspects of the brain by some appropriate computational models [1].

Cellular Automaton (CA) is a mathematical tool to model systems with many simple elements working together and creating a global evolutionary pattern of behavior [2]. The CA, firstly introduced by Stanislaw Ulam and John von Neumann in 1940s, went under more systematic study by Stephen Wolfram in 1980s. A classic CA is created from N cells, each of them having one of the predefined discrete possible states (e.g. 0 and 1) in each evolutionary time step. Cells take effect from a pre-defined neighborhood around them and can change their initial state into the next state based upon an "interaction rule" with respect to their neighborhood. Nowadays, more generalized versions of the CA are becoming popular, such as probabilistic CA, continuous CA, CA with dynamic rules, etc. [3].

Employing CA in the field of neuroscience has shown successful results in the interpretation of some cognitive aspects of the brain [4-8]. Compared to other computational models, such as Artificial Neural Networks (ANN), Spiking Neural Networks (SNN), Coupled Neural Networks (CNNs), and Globally Coupled Maps (GCM), a cellular automaton could be considered as a more general form since it is capable to have properties of all the above-mentioned approaches.

We have proposed that an appropriate form of CA could be used in modeling the *visual perceptual dynamics* [9]. In this paper, we show that by considering the real anatomical connections among the brain networks and using them carefully in the structure of CA, a well representative model for visual perception can be represented, both structurally and dynamically.

It has already been demonstrated that brain dynamics (which are reflected in EEG, MEG, and ECoG signals) are inherently chaotic [10]. As we

*. *Corresponding author. Tel.: +98 21 64542370*
E-mail addresses: mbeigzadeh@aut.ac.ir (M. Beigzadeh); mrhashemigolpayegani@aut.ac.ir (S.M.R. Hashemi Golpayegani)

perceive different sensory information (i.e. scenes, sounds, odors, etc.) and recognize different patterns, these dynamical processes tend to turn into a more regular pattern. This stage has been referred by other researchers as: "the transients between gas-like randomness and liquid-like order" [11]. According to such paradigm, each stimulus would tend to lead the system to its own "liquid-like attractor". Liquid-like attractors, corresponding to each stimulus, are different from each other. Therefore, after the sensorial stimuli, the brain dynamics would start a search in its general chaotic basin of attraction and finally release into its appropriate attractor and recognize that special stimulus.

The proposed computational model tries to maintain these attractors and show the possibility of dynamical transitions between them by changing the parameter values of the model or the initial condition. Since the structure of the proposed model is tried to be imitated from the structure and connections of the visual system, those dynamical behaviors produced by the model could be related to visual dynamics. When a visual stimulus comes, the "visual pathways" will interact with that stimuli and will make responses that create those kinds of global dynamical behaviors.

The most important property of CA in modeling complex multi-agent systems is its ability to imitate the "interaction" between those agents to some extent. It means that in the CA, we are able to define and adjust different (mostly simple) interaction rules among the agents. In this way, we can make each agent "bifurcate" and change patterns of behavior. Interactions among the neural networks of the brain may result into many perceptual, cognitive, and motor behaviors.

Connectivity plays an important role in large networked dynamical systems [1]. That is why in biological systems (such as brain networks) the structural (anatomical) and the functional connectivity patterns are being studied with great interest [12-15]. In modeling approaches, we should firstly determine the connection pattern and relationships between the elements and then define how these – anatomically/functionally – connected networks could make the dynamical behavior of each element and the whole network evolve in time. In this work, we adopt the real anatomical connection matrix of the macaque visual system for our modeling (the work published by Felleman and Essen [16]).

The remainder of this paper is organized as follows: In Section 2, we will introduce our proposed model completely. The main structure of the network and its elements are illustrated in Section 2.1, and then in Sections 2.2 through 2.4, more details are discussed which include: in-layer and between-layer connections, interaction rules of the CA, and finally, the way of considering delays in the network.

Section 3 contains the numerical results and simulations of the model. The numerical studies are based on presenting the time series, phase portraits and bifurcation diagrams, and frequency content and synchronization patterns of the network, in different conditions, trying to show the capabilities of the model to mimic the visual perceptual dynamics (chaotic and other types of more regular attractors). Finally, in Section 4, we will have the conclusion and more discussions about the whole proposal.

2. The proposed model

In this section, we introduce our model of visual perception using anatomical connectivity matrix on a cellular automaton platform. This model tries to mimic the dynamical behaviors that happen during visual perceptual states. As mentioned before, we are going to use an anatomical connectivity matrix of the macaque visual cortex in our modeling, which has been extracted from the study of Essen and Felleman [16]. The result of their study on macaque visual cortex was a 35×35 connection matrix (see Appendix A) corresponding to different cortical areas in the occipital, temporal, parietal, and frontal cortex of the macaque. This 35×35 connection matrix was then modified into a simpler 30×30 one by Sporns (this connection matrix could be downloaded from: https://sites.google.com/site/bctnet/datasets) [17] in which the uncertain and not-connected pathways has been omitted. In the new modified and simplified connection matrix, each element could be equal to 0 or 1. Zero values denote a "no-connection" situation, and non-zero ones correspond to a valid connection between two nodes. This connection matrix has shown to have the "small world" properties which is necessary for the brain to show many of its functional properties, such as synchronization [18].

The building blocks of our model are chosen to be of a well-known dynamical model: the logistic map (Eq. (1)), in order to represent "netlets" (populations of 100-1000 excitatory and inhibitory neurons). Netlets were introduced by Hrath in 1970 to describe the activation of an excitatory-inhibitory population of neurons in the cortex [19-20]. Later, this concept was used in a computational model for visual cortex by Pashaie and Farhat [21]. In their approach, each netlet is supposed to work as a Complex Processing Element (CPE) which is modeled by the logistic map:

$$X(n+1) = pX(n)\left(1 - X(n)\right). \tag{1}$$

The reason for using logistic map as the model of a netlet's dynamics is discussed here. It has been shown that the expectation value of netlet activity could be modeled by Eq. (2) [19-20]:

$$< a_{n+1} > \cong (1-\alpha_n) \times \left(\exp[-\alpha_n h \mu^-] \sum_{m=0}^{M} \left\{ \frac{(\alpha_n h \mu^-)^m}{m!} \right\} \right) \times \left(1 - \exp\left[-\alpha_n (1-h)\mu^+\right] \sum_{l=0}^{\eta'-1} \left\{ \frac{[\alpha_n (1-h)\mu^+]^l}{l!} \right\} \right). \quad (2)$$

In this formulation, α_n is the activation of an isolated netlet at time step n, and $< \alpha_{n+1} >$ is its expected value at time step $n+1$. Parameter h stands for the fraction of inhibitory neurons in the netlet, μ^+ (and μ^-) is the average number of neurons in the netlet with afferent connections from a given excitatory (inhibitory) neuron in the netlet. Parameter η' is the minimum number of excitatory and inhibitory inputs necessary to trigger a neuron which has received m inhibitory inputs, and finally, M is the total number of inhibitory connections [21].

Graphs of $<\alpha_{n+1}>$ versus α_n for a netlet with the same amount of excitatory and inhibitory connections "$\mu^+ = \mu^- = 10$" and "$h = 0.3$" are shown in Figure 1(a). It can be seen that the shapes of these curves could be considered very similar to the plots of the well-known logistic map, for normalized p parameters between 0 and 1 (Figure 1(b)).

2.1. The main structure of the network and its elements

Based on the anatomical connections described before, our model is considered to have 30 layers, each corresponding to one of the areas in the occipital, temporal, parietal, and frontal cortex (in summary, in the visual system) of the macaque brain (see Appendix A). There are N dynamical agents corresponding to N netlets in each layer. The generalized form of coupled logistic maps would be:

$$x_{l,m}(n+1) = p_{l,m} x_{l,m}(n) \left(1 - x_{l,m}(n)\right),$$
$$l = 1, ..., 30, \qquad m = 1, ..., N,$$
$$p_{l,m} = f \text{ (neighbors of element } x_{l,m}), \quad (3)$$

in which $x_{l,m}(n)$ corresponds to the activation of element m in layer l, at time step n, and $p_{l,m}$, the coupling factor, is a function of its neighbors' activities.

Note that the parameter p (the environmental parameter) is the main source of changing dynamics (and creating bifurcations) in the conventional logistic map (Eq. (1)) which can make period-1, period-2 ... and chaotic attractors (see the bifurcation diagram of Figure 2). Therefore, it is clear that if we want to model the "interactive" effects of "the environment" on each agent of the network, we have to change the value of $p_{l,m}$ in an appropriate manner for each agent (based on the activities of the other affecting agents on it).

2.2. Inter-layer and intra-layer connections

The relationships between layers are determined by the connection matrix C (Appendix A). In this way, if two layers are connected to each other, the value of C is considered to be 1, and if they are not anatomically connected, the corresponding C element will be considered to be 0. But, the connected areas may affect each other not equally. So, we have to attribute a weight or

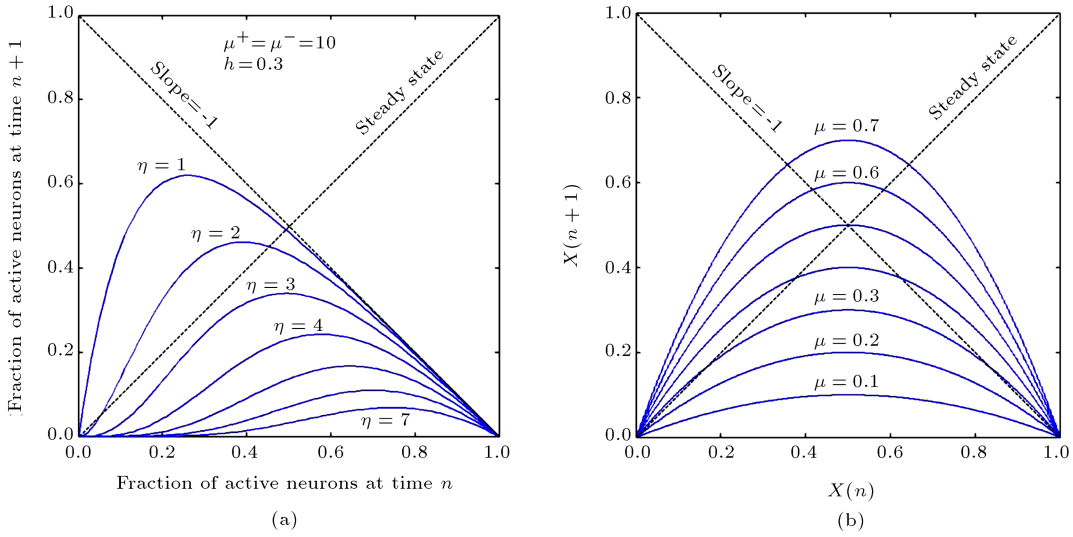

Figure 1. (a) Fraction of the active nodes of a netlet, with the same amount of excitatory and inhibitory connections, at the moment $n+1$ as a function of active nodes at the previous moment. Different curves correspond to different numbers of presynaptic spikes that are necessary to elicit a postsynaptic spike. (b) Group of quadratic functions employed in the generation of the logistic map (in the form of $x_{n+1} = 4\mu x_n(1-x_n)$). The curves in this figure are quadratic functions that are plotted for different values assigned to the bifurcation parameter μ (adopted from [21]).

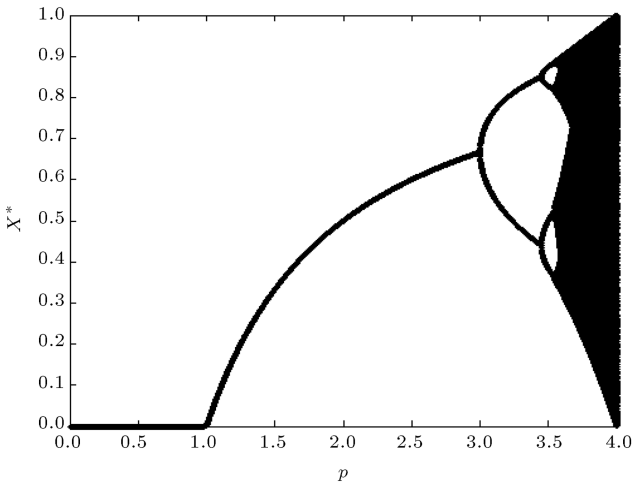

Figure 2. The bifurcation diagram of the conventional logistic map $X(k+1) = pX(k)(1-X(k))$, due to the bifurcation parameter, p.

a strength parameter to those connections in the form of a weight matrix W. These weights are considered to be random values between 0 and 1. Since we have not inserted any learning algorithm in this model yet, these weights are considered to be fixed during the CA evolution.

We also tried to make the model closer to the reality by considering both excitatory and inhibitory connections between the agents. It is well-known that the balance between excitatory and inhibitory neurons in the cortex is almost 70-30% [22], or 80-20% [23-24], respectively. Therefore, among all connections, 80% were considered to be excitatory and 20% to be inhibitory.

It also should be emphasized that although the number of inhibitory connections is less than that of the excitatory ones, the inhibitory synapses play a very important role in the behavior of the brain. That is why we considered the amplitudes of the inhibitory weights to be larger than those of the excitatory ones (in the order of 7-8 times larger) to take their importance into account. The same concept has also been reported in other related works [1].

2.3. Interaction rules

As it was discussed earlier, the most important part of CA based modeling is the determination of interaction rules among the agents. We mentioned at the end of Section 2.1 that if we want to simulate the effect of environment on each logistic-type agent, we would better change the value of $p_{l,m}$ of element m in layer l.

Based on the bifurcation diagram of Figure 2, in the conventional logistic map (Eq. (1)), if $p > 3.56$ (for example $p = 4$), chaos is observed (which can be interpreted as a model of chaotic bursts seen in the active state of neural populations), and if $p = 1$, a stable period-1 behavior is achieved which can be related to the fully recognizing state of the netlet [21].

This was used by Lopez et al. to construct their interesting interaction rule among the logistic-type agents in the modeling of bi-stability in the brain [4]. Lopez used two linear relationships in order to simulate the excitatory and inhibitory forms of interaction as follows:

Lopez interaction rules [4]. For agent i of the N elements in a network, we have $x^i_{n+1} = \bar{p}_i x^i_n(1-x^i_n)$, in which the value $\bar{p}_i$ is the effect of other N_i neighboring elements on x^i_n. This net-effect could be excitatory or inhibitory. This function is selected to be a linear function depending on the actual "local mean value", X^i_n of the neighboring signal activity, and expanding the interval $p_i \in [0,1]$ into $\bar{p}_i \in [0,4]$ in the form below:

$$\begin{cases} \bar{p}_i = p_i(3X^i_n + 1) & \textit{Excitation coupling} \\ \bar{p}_i = p_i(-3X^i_n + 4) & \textit{Inhibition coupling} \end{cases} \quad (4)$$

in which $X^i_n = round(\frac{1}{N_i}\sum_{j=1}^{N_i} x^j_n)$ is inherently a Boolean operator comparing $\frac{1}{N_i}\sum_{j=1}^{N_i} x^j_n$ with threshold 0.5 (therefore, the value of X^i_n could only be equal to 0 or 1).

In this way, the values of $(3X^i_n+1)$ and $(-3X^i_n+4)$ will always be either 1 or 4, based on the mean activities of the neighbors and their interaction type (i.e. excitation or inhibition). Therefore, the interaction of neighbors could make the target agent become silent (when $\bar{p}_i = 1 \times p_i$) or become active in a bursting pattern (when $\bar{p}_i = 4 \times p_i$). Different dynamical behaviors for each element could be reached by changing the value of p_i between [0,1] as the bifurcation parameter.

Most of the researchers, like Lopez, have used those rules in a "fully excitatory or fully inhibitory" network with random or regular connections. But, here, we have considered our model to be more realistic, structurally in four aspects:

1. Having 80% excitatory and 20% inhibitory netlets (based on physiological data), instead of fully excitatory or fully inhibitory networks;
2. Using the anatomical connections which, compared to a completely ordered or a fully random network, have a more similar connectivity pattern to the brain and have proved to have small world properties [18,25];
3. Adopting a weighted matrix as inter-layer and intra-layer coupling strength among netlets, instead of considering all connections to be identical;
4. Considering some time delays among netlets (see Section 2.4) based on synaptic delays.

However, the most important and novel difference of our proposed model, compared to other similar models of neural dynamics, is the way we define "interaction rules" among those agents in the evolution of our CA:

The proposed interaction rules. We use a modified version of the idea of coupled logistic maps in a completely different framework, which we think is a more realistic one, using a "multiplicative relationship" and a "geometric mean" instead of the popular "additive relationship" and "arithmetic mean", to model the total effect of the neighbors on each agent.

For an element x_n^i in a network of N coupled logistic-type agents, we have:

$$x_{n+1}^i = \bar{p}_i * x_n^i * (1 - x_n^i).$$

The net effect of excitatory-inhibitory connections from the neighbors is reflected in the value of $\bar{p}_i$ in the form of:

$$\bar{p}_i = p_i \left(\sqrt[(N_{ecx}+N_{inh})]{\Pi_{j=1}^{N_{ecx}} X_{j,exc}^i * \Pi_{j=1}^{N_{inh}} X_{j,inh}^i} \right). \quad (5)$$

This is a "geometric mean" among the neighbors!

We will discuss later that the geometric mean could be a more realistic form of interaction in our model. We borrow a modified version of the definition of excitation and inhibition from the work of Lopez [4]:

$$\begin{cases} X_{j,exc}^i = \left(3(x_n^i > th_e) + 1\right) & \textit{Excitation coupling} \\ X_{j,inh}^i = \left(-3(x_n^i > th_i) + 4\right) & \textit{Inhibition coupling} \end{cases}$$

Therefore, instead of using the very popular threshold value "0.5" in the Boolean operator like this:

$$round(x_n^j) = (x_n^j > 0.5).$$

We suggest using two different "adaptive" threshold values of th_e and th_i for excitatory and inhibitory synapses, respectively. This could be generally more realistic, because there is no reason that all synapses have the same threshold of $th = 0.5$ to start activation. Besides, we do this comparison for "each neighbor" independently, compared to the work of Lopez in which the "arithmetic mean" of the neighbors was compared to the threshold.

The output values of $X_{j,exc}^i$ (and $X_{j,inh}^i$) for each neighbor could be equal to 4 or 1 (1 or 4) based on the values of x_n^j, th_e, and th_i, and also the predefined type of the connections (excitatory or inhibitory). Therefore, by selecting $p_i \in [0, 1]$, we will have $\bar{p}_i \in [0, 4]$.

We believe that the geometric mean is a more realistic interaction rule than the arithmetic mean in our application. Here, we are going to discuss this issue. Consider we want to affect a logistic-type agent (change its dynamical behavior) by changing its environmental parameter, p. Consider this element has N_{inh} inhibitory and N_{ecx} excitatory neighbors. If we use an arithmetic model of interaction, we simply have to use the-weighted-sum of all excitatory-inhibitory effects as follows:

$$X_n^i = \left| \frac{1}{N_{ecx}} \sum_{j=1}^{N_{ecx}} w^j x_n^j - \frac{1}{N_{inh}} \sum_{j=1}^{N_{inh}} w^j x_n^j \right|. \quad (6)$$

And use it in a suitable coded form in the logistic equation, like Eq. (4). But this form of mean value fades or degrades the independent effect of each individual neighbor on the target element xi. However, when a multiplicative interaction in the form of a geometric mean is used, each neighbor is compared to its own threshold value and after that, it could affect the target directly. This effect could be studied, independently of others without being faded or degraded by them, since all of them take part in the final production as:

$$X_n^i = \sqrt[(N_{ecx}+N_{inh})]{\Pi_{j=1}^{N_{ecx}} X_{j,exc}^i * \Pi_{j=1}^{N_{inh}} X_{j,inh}^i}.$$

Another potential advantage of this form of coupling is its capability to create complex behaviors of the neural populations because of its "nonlinearity", as the whole system is highly nonlinear (compare this with the simpler linear weighted sum of Eq. (6)).

2.4. Time delays

Timings of the activation and inactivation of neurons play a very important role in the overall dynamics of the whole system [26]. This is mainly because of the synaptic delays. On one hand, most of the computational neuroscientists discard delays as some unimportant thing that only complicates modeling. From a mathematical point of view, a system with delays is not finite -but infinite- dimensional which poses some mathematical and simulation difficulties [26]. On the other hand, others argue that an infinite dimensionality of spiking networks with axonal delays is not a disadvantage, but an immense advantage that results in an unprecedented information capacity. Izhikevich even claims that there are some stable firing patterns that are not possible without those delays [26]. Neither are we going to neglect the intrinsic role of the delays in the neural system.

In the original form of netlets' activation function (Eq. (2)), for which we used logistic equation as the model, the time has been quantized in units of the synaptic delay τ, and it is assumed that the neurons can fire only at times which are integral multiples of [20]. Therefore, each discrete time step in the logistic map refers to the continuous time interval of τ. Hence, the discrete value of n corresponds to $t = n\tau$ in the

continuous time scale. But what is the value of τ itself?

Some researchers argue that the synaptic delays and the refractory periods generally are found to be close to 0.5 ms and 1 ms, respectively [20]. Another report about this quantity is of the order of 1-3 ms [1]. But the report of Izhikevich from the synaptic delays seems more realistic, since it covers a broader interval and talks mainly about the neocortex: "A careful measurement of axonal conduction delays in the mammalian neocortex showed that they could be as small as 0.1 ms and as large as 44 ms, depending on the type and location of the neurons" [26].

In our work, we considered the specific value of $\tau \approx 10$ ms as the "mean" time interval between two activations. This value is important and mainly adopted because we are going to use the time delays present "between" processing layers of the visual system in our model. The latencies between the processing layers of the ventral pathway in the visual system have been reported in [27,28] and could be seen schematically in Figure 3. We used this platform in order to estimate the other latencies between the layers of our model.

It should be emphasized here that although our model is a behavioral and functional one, we are trying to use as much structural and physiological data as possible, because in any complex system, the structure could not be separated from the function. Based upon the above discussion and by using the data in Figure 3 and the connection matrix of macaque visual cortex, we estimated the other between-layer latencies in the form of discrete time steps of our logistic-type model (see Table 1).

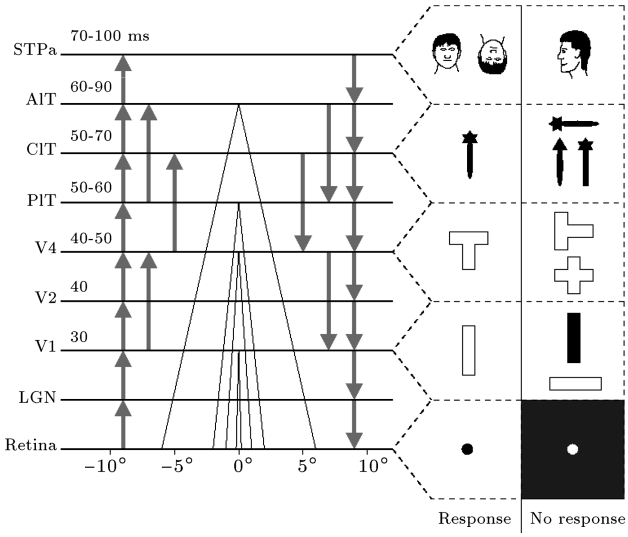

Figure 3. Latencies between the layered structure of the ventral pathway (from retina to STPa) in milliseconds (adopted from [28]).

By using the above updating rules for each element of our cellular automata, we are now ready to simulate the proposed model and validate some of our

Table 1. Travel time from retina to different visual processing layers of our model (first row: in mili-seconds, second row (k-steps): in the discrete time interval, normalized to the time unit $\tau = 10$ ms). The bold columns contain the exact values from Figure 3; other columns are estimated based on the bold ones: (a) Occipital cortex, (b) temporal cortex, and (c) parietal and frontal cortex.

(a)

Occipital									
From retina to:	**V1**	**V2**	V3	**V4**	VIA	V4	VOT	V4L	MT
ms	**30**	**40**	42	**43** **40-50**	43	45	46	46	48
k-steps	**3**	**4**	4	**4**	4	5	5	5	5

(b)

Temporal											
From retina to:	**FST**	**PITd**	**PITv**	**CITd**	**CITv**	**AITd**	**AITv**	STPp	**STPa**	TF	TH
ms	**50**	**50** **50-60**	**55** **50-60**	**60** **50-70**	**65** **50-70**	**70** **60-90**	**80** **60-90**	75	**90** **70-100**	100	100
k-steps	**5**	**5**	**6**	**6**	**7**	**7**	**8**	8	**9**	10	10

(c)

	Parietal								**Frontal**	
From retina to:	MSTd	MSTI	PO	PIP	LIP	VIP	DP	7a	FEF	46
ms	100	100	100	100	100	100	100	100	100	100
k-steps	10	10	10	10	10	10	10	10	10	10

Table 2. The simulation framework and the selected values of parameters.

Parameter	Value	Parameter	Value
Number of layers	30	Connection weights	Random values in the [0,1] interval
Connection matrix between layers	30×30 C, from macaque visual cortex	Inhibitory to excitatory weights ratio	7-8
Number of netlets in each layer	$N = 5$	Mean synaptic delays (in-layer delays)	10 ms
Ratio of excitatory to inhibitory synapses	4	Between layers latencies	Based on Table 2
p	Identical for all agents, changing from 0 to 1	Interaction rule	Geometric mean
		th_i	0.05
		th_e	0.8

statements about the applicability of such a model in mimicking the visual perceptual dynamics.

3. Simulation results

The summary of our selected values of parameters and the global framework of modeling are shown in Table 2. Under these situations, the whole model is capable of showing different kinds of dynamical behaviors and attractors depending on different perceptual situations.

In our first experiments, we supposed that all agents in all layers were in the form of Eq. (3), in which $p_{l,m} = \bar{p}_i$ from Eq. (5), and they all had the same value of parameter $p_j = p$ (see Eq. (5)). Then, we studied different behaviors of the CA using the bifurcation diagram due to parameter p. After that, different values of $p_{l,m}$ were studied in the model. The output value selected for this model is considered to be "the mean activation of the whole network in each iteration" as an estimation of cortical electrical activities recorded by the EEG or ECoG electrodes [11]. We also study the synchronization and desynchronization properties of the netlets using correlation values in different environmental situations [11,29]. The detailed results are presented in the following sub-sections.

3.1. Different dynamics, bifurcation diagram

The bifurcation diagram of CA under the conditions described in the previous sub-section is presented in Figure 4. Here, all of the agents are considered to have the same value of p. The network starts from some random initial conditions and evolves to its attractor after 500 iterations. We use the last 200 samples as the attractor (i.e. omit the first 300 samples as the transient part). CA update is performed synchronously. It can be seen from the bifurcation diagram that the system is capable of showing different dynamical states which any of them could be interpreted as one of the widespread perceptual states of the visual system.

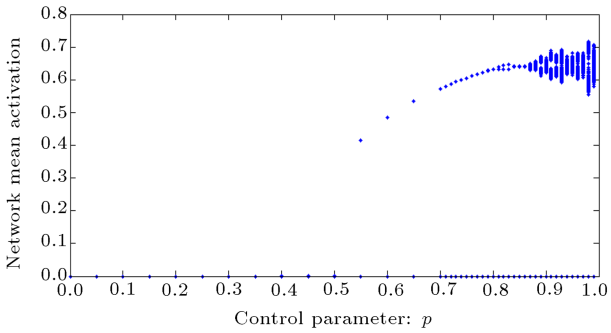

Figure 4. Bifurcation diagram of the CA as a function of control parameter, p (threshold values are set to $th_i = 0.8$, $th_e = 0.05$). The values of p are scanned with 0.05 steps from $p = 0$ to $p = 0.7$ in order to save time and with 0.01 steps from $p = 0.71$ to $p = 0.99$, in order to observe more details. The CA is evolved for 500 iterations for each value of p, and the final 200 samples are plotted (i.e. 300 samples are considered as transient). The bifurcation diagram is plotted for random initial conditions.

In Figure 5(a), the CA shows a period-1 behavior around $p = 0.7$. This period-1, or fixed point behavior, could be representative of a state in which the visual system settles into a fixed attractor, i.e. recognizes a stimulus. Figure 5(b), on the other hand, shows a period-2 situation for $p = 0.83$ which can be a model of bi-stable perception. Bi-stability and multi-stability, in general, is an interesting phenomenon studied in the literature with great interest in recent years [4,30,31].

For example, a bi-stable perception can happen in the visual system of a person, while he/she is looking at the simple shape of Figure 6. In this shape, the perceptual dynamics switch between the image of "two faces" and the image of "a vase" in the middle part. Any of these perceptions can be modeled as one of the stable states in the period-2 region of CA. The perceptual system of the brain switches between these two stable points in a periodic way which represents the period-2 solution. The more complex situation of

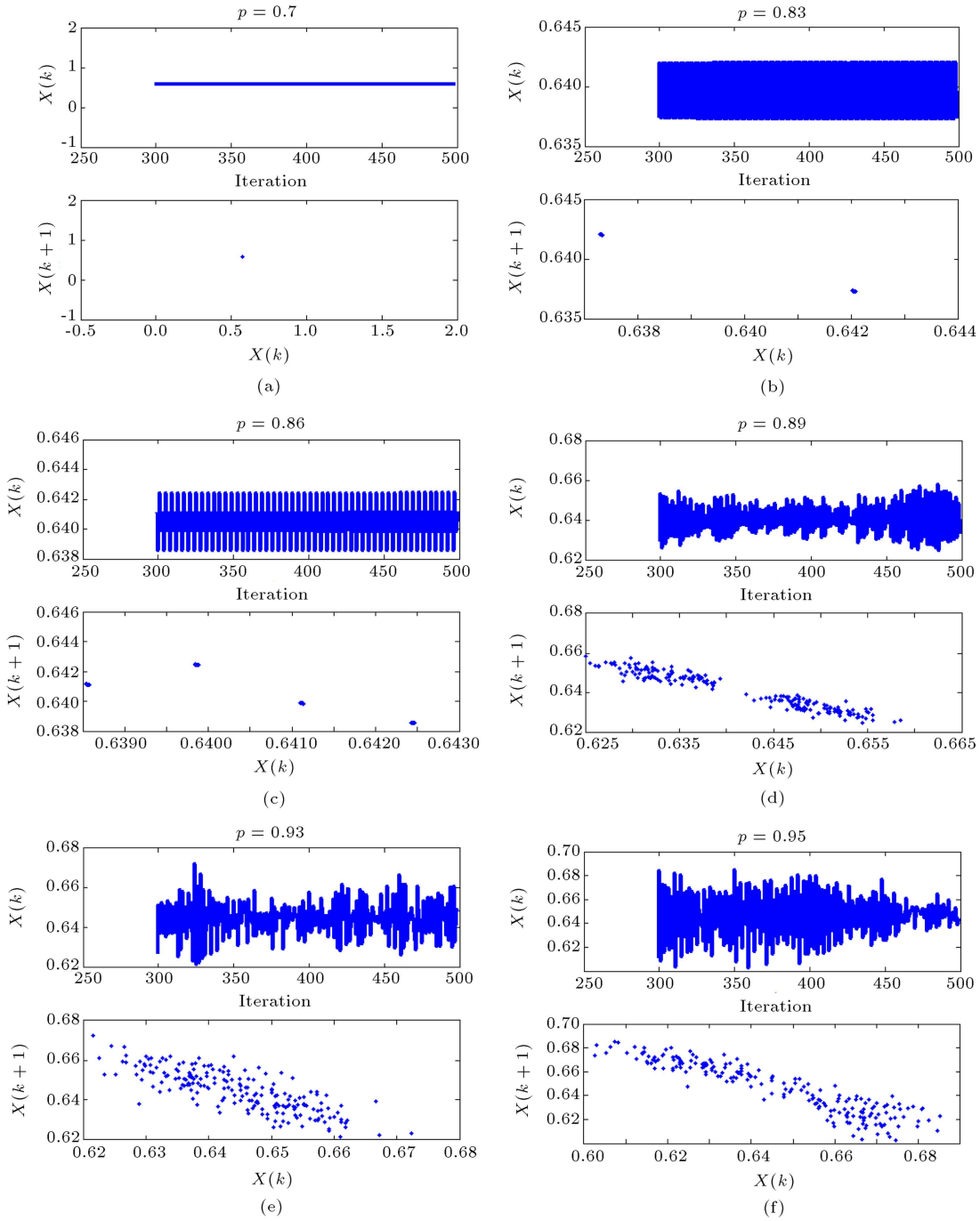

Figure 5. Different dynamical behaviors of the CA for 500 iterations from the initial condition (for threshold values of $th_i = 0.8$ and $th_e = 0.05$). Top plot: the time series (by omitting first 300 samples as the transient part), Bottom plot: the phase portrait (i.e. $x(k+1)$ versus $x(k)$): (a) Period-1 for $p = 0.7$; (b) period-2 for $p = 0.83$; (c) period-4 for $p = 0.86$; (d) two-part non-periodic attractor for $p = 0.89$; and (e)-(f) chaotic attractors for $p = 0.93$ and $p = 0.95$, respectively.

period-4, which is indicative of a 4-stable situation, occurs for $p = 0.86$ (Figure 5(c)).

But the most interesting behaviors can be seen in Figure 5(d)-(f) as the non-periodic cases. It can be seen in Figure 5(d) that for $p = 0.89$, a two-part non-periodic attractor appears which could be interpreted as a "blur" bi-stable perception of a stimulus, or a 2-tori quasi periodic response when our visual system has not reached a single decision about a stimulus and is searching around two possible answers!

Figure 5(e) and (f) show a chaotic attractor. We can interpret this attractor as the baseline behavior of the brain, when it has not been encountered with a new stimulus. This baseline is the main dynamical state of the brain, from which it could be attenuated due to an external stimuli (scene, odor, etc.). Hence,

Figure 6. A bi-stable perceptual situation could occur by the visual system in the observation of this simple shape: a vase or two faces? This bi-stability could be modeled by the period-2 behavior of the CA model.

in the presence of an external stimulus, this attractor changes into one (or some) ordered attractor(s), called liquid-like quasi-attractors, corresponding to that specific stimulus [10,11]. Then, it again comes back to this baseline chaotic attractor in order to be ready to interact with the next and next changes in the environment. The real chaotic dynamic of the brain could be interpreted as the searching state of the brain in its basin of attraction, coming into and going beyond the chaotic and non-chaotic attractors.

It could be seen in Figure 7 that the frequency content of this chaotic signal is comparable with the $\frac{1}{f^{\alpha}}$, $\alpha \approx 2$ spectrum that is seen in the normal EEG signal [8].

3.2. A more realistic situation

In the previous part, like many other related works [4,21], we assumed that all of the agents have the same bifurcation parameter p (that is $\forall j p_j = p$ in Eq. (5), which then would be used in Eq. (3) in the form of $p_{l,m} \equiv \bar{p}_j$). Indeed, this could not be the real situation; there is no reason for all neural populations to have the same value of p in general. Rather, the dynamical state and properties of each neural population may be different from the others. Hence, a more realistic approach in modeling is to consider each agent to have its own value of p which is not necessarily equal to those of the other agents.

In order to do that, we considered some random values for parameter p of each agent ($p \in [0, 1]$). The result could resemble the behavior of real EEG signals in the form of its spectra and the synchronization-desynchronization patterns of 150 agents. This can mimic the functional relationships and synchrony among different neural populations of the visual system (Figure 8). We should emphasize that we are not talking about the synchronization of the whole network; rather we are talking about the occurrence of some "transient synchrony" among "a number of neural populations", not all of them. These partial synchronization-desynchronizations of neural populations maintain the whole dynamical behavior of the brain.

The synchronization pattern is calculated between each agent and the mean activation of the network (the ensemble), in a window size of 50 samples, for a total size of 450 iterations (by the "xcorr" Matlab function) [29].

4. Conclusion

A model of visual perceptual dynamics based on cellular automata was introduced. The model is a behavioral and phenomenological model which tries to take into account as much physiological and anatomical considerations as possible, such as anatomical connection matrix of macaque visual cortex, netlet dynamics, excitatory-inhibitory synapses with appropriate ratio and weights, in-layer delays and between-layer

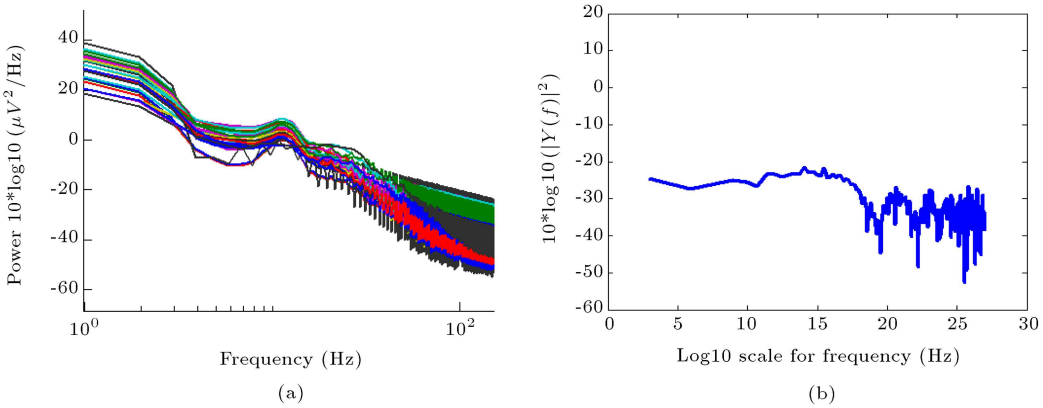

Figure 7. (a) EEG spectra for different EEG electrodes, recorded in a visual task. (b) The spectra of the chaotic output signal of CA, for $p = 0.95$, which could be considered to have a $\frac{1}{f^{\alpha}}$ form, comparable with the normal EEG.

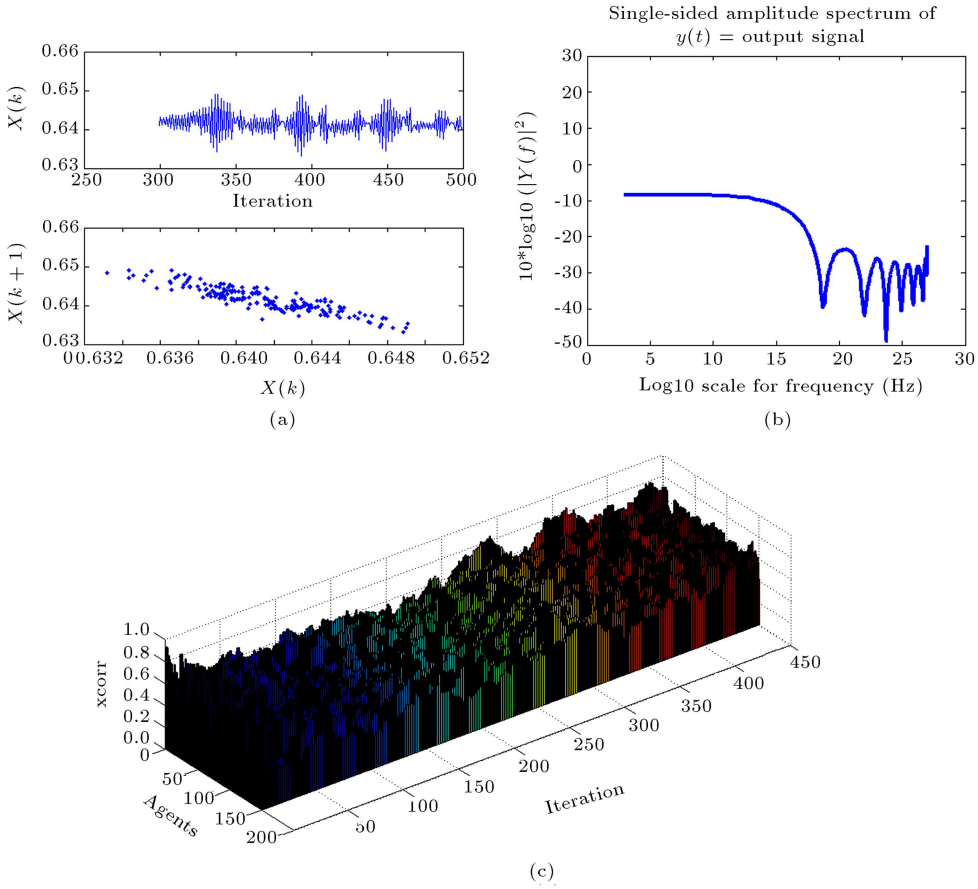

Figure 8. (a) The time evolution and the phase portrait of the chaotic output signal of CA with different values of parameter p for each agent (values are selected randomly between 0-1). (b) The spectra of part (a). (c) The synchronization-desynchronization pattern of all agents during the evolution of CA in 450 steps, in terms of correlation coefficient measure using a 50 step window.

latencies. This model is one of the most complete models proposed for neural dynamics which considers anatomical connections in combination with a CA approach using chaotic maps.

One of the most important advantages of using CA for our modeling was cellular automaton, a modeling tool capable of modeling large scale complex systems which gives the ability to study the system from microscopic to mesoscopic and macroscopic levels. It also makes it possible to define and tune the appropriate interaction rules in order to reach the desired behavior for the whole system.

We introduced a new interaction rule based upon the "geometric mean" value (a nonlinear synaptic function) and multiplicative relationship among the agents. We claim that it can be more realistic than the previous arithmetic mean and linear interaction rules, because it gives the possibility of changing and studying each neighbor, individually, without being degraded by the others. We also used adaptive thresholds in our synaptic decision makings. We should clarify here that the meaning of "adaptability in thresholds" in our paper is that we did not limit ourselves to use only the popular threshold of 0.5. We would rather choose different values of threshold for excitatory and inhibitory synapses which are not necessarily equal to 0.5.

It was shown that the proposed model was capable of showing different dynamical behaviors seen in visual perceptual framework, from a fixed stable attractor to bi-stable, multi-stable, and chaotic behaviors. The chaotic signal was shown to have a $\frac{1}{f^{\alpha}}$ form of frequency spectrum comparable with the spectrum of a normal EEG. We also showed that the synchronization-desynchronization pattern of the agents in their evolution could resemble - visually - the real patterns seen among EEG electrode signals during visual tasks.

The future works on this model should consider the effects of learning and seeing different scenes on the model parameters, based on a suitable learning approach such as STDP. It may also be developed by considering two-dimensional CAs instead of current one-dimensional form, for each layer. Besides, some visual perceptual deficits, such as face recognition problems, seen in the Autism disorder may be behaviorally modeled by this model in the future.

References

1. Barbosa, M., Dockendorf, K., Escalona, M., Ibarz, B., Miliots, A., Nadal-Sendina, I., Zamora-Lopez, G. and Zemanava, L. "Parallel computation of large neuronal networks with structured connectivity", In: *Lectures in Supercomputational Neuroscience: Understanding Complex Systems*, 1st Edn., Chapter 14, pp. 343-367, Springer-Verlag Berlin Heidelberg (2008).

2. Packard, N.H. and Wolfram, S. "Two-dimensional cellular automata", *J. Stat. Phys.*, **38**(5/6). pp. 901-946 (1985).

3. "Cellular automaton", Wikipedia, the free encyclopedia, 3 September 2014. [Online].
Available: http://en.wikipedia.org/wiki/Cellular_automaton. [Accessed 27 10 2014].

4. Lopez-Ruiz, R. and Fournier-Prunaret, D. "The bistable brain: A neuronal model with symbiotic interactions", In: *Symbiosis, Evolution, Biology and Ecological Effects*, Camisão, A.F., and Pedroso, C.C., Eds., pp. 235-253 (2013).

5. Kozma, R. and Pulji, M. "Hierarchical random cellular neural networks for system-level brain-like signal processing", *Neural Netw.*, **45**, pp. 101-110 (2013).

6. Adams, F.R., Nguyen, H.T., Raghavan, R. and Slawny, J. "A parallel network for visual cognition", *IEEE Trans. Neural Netw.*, **3**(6), pp. 906-922 (1992).

7. Mattei, T.A. "The fuzzy logic of degenerative disc disease: From a Lorenz attractor to a percolation threshold model", *World Neurosurg.*, **80**, pp. 8-12 (2013).

8. Kozma, R. and Puljic, M. "Chaotic behavior in probabilistic cellular neural networks", *The International Joint Conference on Neural Networks (IJCNN)*, Barcelona, Spain, pp. 1-7 (2010).

9. Beigzadeh, M., Hashemi Golpayegani, S.M.R. and Gharibzadeh, S. "Can cellular automata be a representative model for visual perception dynamics?", *Front. Comp. Neurosci.*, **7**(130), pp. 1-2 (2013).

10. Freeman, W.J. "The physiology of perception", *SCI AM*, **264**, pp. 78-85 (1991).

11. Kozma, R., Pulji, M. and Freeman, W.J. "Thermodynamic model of criticality in the cortex based on EEG/ECOG data", In: *Criticality in Neural Systems*, Chapter 1, Berkeley, John Wiley & Sons, Inc., pp. 1-22 (2012).

12. Ponten, S.C., Daffertshofer, A., Hillebrand, A. and Stam, C.J. "The relationship between structural and functional connectivity: Graph theoretical analysis of an EEG neural mass model", *NeuroImage.*, **52**, pp. 985-994 (2010).

13. Sporns, O. "Small-world connectivity, motif composition and complexity of fractal neuronal connections", *BioSystems*, **85**, pp. 55-64 (2006).

14. Stam, C.J. and Reijneveld, J.C. "Graph theoretical analysis of complex networks in the brain", *Nonlinear Biomed. Phys.*, **1**(3), pp. 1-19 (2007).

15. Sporns, O. "Contributions and challenges for network models in cognitive neuroscience", *Nat. Rev. Neurosci.*, **17**, pp. 652-660 (2014).

16. Felleman, D.J. and Van Essen, D.C. "Distributed hierarchical processing in the primate cerebral cortex", *Cereb. Cortex*, **1**, pp. 1-47 (1991).

17. Sporns, O. "Connectivity network data sets - Brain connectivity toolbox", (2000).
Link: https://sites.google.com/site/bctnet/datasets. Accessed: 12/10/2015.

18. Sporns, O. and Zwi, J.D. "The small world of the cerebral cortex", *Neuroinform.*, **2**, pp. 145-162 (2004).

19. Anninos, P.A., Beek, B., Csermely, T.J., Harth, E.M. and Pertile, G. "Dynamics of neural structures", *J. Theor. Biol.*, **26**, pp. 121-148 (1970).

20. Harth, E.M., Csermely, T.J., Beek, B. and Lindsay, R.D. "Brain functions and neural dynamics", *J. Theor. Biol.*, **26**, pp. 93-120 (1970).

21. Pashaie, R. and Farhat, N.H. "Self-organization in a parametrically coupled logistic map network: A model for information processing in the visual cortex", *IEEE Trans. Neural Netw.*, **20**(4), pp. 597-608 (2009).

22. Chen, X. and Dzakpasu, R. "Observed network dynamics from altering the balance between excitatory and inhibitory neurons in cultured networks", *Phys. Rev. E.*, **82**, pp. 1-19 {031907} (2010).

23. King, P.D., Zylberberg, J. and DeWeese, M.R. "Inhibitory interneurons enable sparse code formation in a spiking circuit model of V1", *BMC Neuroscience*, **13**(1), pp. 148-149 (2012).

24. Metaxas, A., Maex, R., Steuber, V., Adams, R. and Davey, N. "The effect of different types of synaptic plasticity on the performance of associative memory networks with excitatory and inhibitory subpopulations", In: *Lecture Notes in Computer Science* (including subseries *Lecture Notes in Artificial Intelligence and Lecture Notes in Bioinformatics)*, pp. 136-142, Springer-Verlag, Berlin, Heidelberg (2012).

25. Rubinov, M. and Sporns, O. "Complex network measures of brain connectivity: Uses and interpretations", *NeuroImage*, **52**, pp. 1059-1069 (2010).

26. Izhikevich, E.M. "Polychronization: Computation with spikes", *Neural Comput.*, **18**, pp. 245-282 (2006).

27. Oram, M.W. and Perrett, D.I. "Modeling visual recognition from neurobiological constraints", Special issue on: *Models of Neurodynamics and Behavior, Neural Networks*, **7**(6/7), pp. 945-972 (1994).

28. Wiskott, L. "How does our visual system achieve shift and size invariance?", In: *23 Problems in Systems*

Neuroscience, van Hemmen, J.L. and Sejnowski, T.J., Eds., Chapter 16, pp. 322-340, Oxford University Press (2006).

29. Puljic, M. and Kozma, R. "Synchrony in probabilistic cellular automata", *Lecture Notes*, University of Memphis, Memphis (2005).

30. Nagao, N., Nishimura, H. and Matsui, N. "A neural chaos model of multistable perception", *Neural. Process Lett.*, **12**(3), pp. 267-276 (2000).

31. Zhou, Y.H., Gao, J.B., White, K.D., Merk, I. and Yao, K. "Perceptual dominance time distributions in multistable visual perception", *Biol Cybern.*, **90**(4), pp. 256-263 (2004).

Appendix A

Table A.1 is a connectivity matrix for interconnections between areas in the macaque visual cortex. Each row shows whether the area listed on the left sends outputs to the areas listed along the top. Conversely, each column shows whether the area listed on the top receives input from the areas listed along the left. (Y) symbols indicate a pathway that has been reported in 1 or more full-length manuscripts. Small plus symbols indicate pathways only in abstracts or unpublished studies. Stars (*) indicate pathways explicitly tested and found to be absent. Blanks indicate pathways not carefully tested. Question marks (?) denote pathways whose existence is uncertain owing to conflicting reports in the literature. "NR" and "NR?" indicate nonreciprocal pathways, i.e. connections absent in the indicated direction, even though the reciprocal connection, has been reported. Shaded boxes along the diagonal represent intrinsic circuitry that exists within each area: These are not indicated among pathways tabulated in the following table, adopted from [16], and reproduced in order to make the resolution better. Green rows and columns are those which are omitted and make the final matrix a 30×30 one.

Table A.1. The 35×35 connectivity matrix of Felleman and Essen [16].

		occipital									Temporal													Parietal									Frontal	
		1	2	3	4	5	6	7	8	9	10	11	12	13	14	15	16	17	18	19	20	21	22	23	24	25	26	27	28	29	30	31	32	33	34	35
		V1	V2	V3	Vp	VIA	V4	VOT	V4l	MT	FST	PITd	PIT	PITv	CITd	CIT	CITv	ATd	ATv	STPp	STP	STPa	TF	TH	MSTd	MSTl	PO	PIP	LIP	VIP	MIP	MCP	DP	7a	FEF	46
1	V1		Y	Y	*	Y	Y	*	NR	Y	*	*		*	*		*	*	*	*		*	*	*	*	?	Y	Y	*	*	*	*	*	*	*	*
2	V2	Y		Y	Y	Y	Y	Y	Y	Y	Y	*		*	*		*	*	*	*		*	*	*	Y	Y	Y	Y	*	Y	*	*	*	*	?	*
3	V3	Y	Y			Y	Y	*	Y	Y	Y	*		*	*		*	*	*	*		*	Y	*	Y	*	Y	Y	Y	Y	*	*		*	?	*
4	Vp	*	Y	Y		Y	Y	Y	*	Y	Y	*		*	*		*	*	*	*		*	Y	*	Y	*	Y	Y		Y	*	*		*	?	*
5	VIA	Y	Y	Y	Y		Y			Y	Y	*		*	*		*	*	*	*		*	*	*	Y	Y	Y				*	*	Y	*	?	*
6	V4	Y	Y	Y	Y	Y			Y	Y	Y	Y		Y	Y		Y	*	Y	*		*	Y	Y	*	*	*	Y	Y	*	*	*	Y	*	?	Y
7	VOT	*	Y	*	Y		Y					Y		Y																						
8	V4l	Y		Y	*		Y			Y	Y														NR?	Y	Y								?	
9	MT	Y	Y	Y	Y	Y	Y		Y		Y	*		*	*		*	*	*	*		*	*	*	Y	Y	?	Y	Y	Y	*	*	*	*	Y	?
10	FST	*	NR?	Y	NR?	Y	Y		Y	Y			Y		*		*	*	*	Y			Y		Y	Y	*	*	Y	Y				Y	Y	*
11	PITd	*	*	*	*	*	Y			*							Y	Y	Y							*	*	*	*	*				*		
12	PIT										Y														Y										Y	Y
13	PITv	*	*	*	*	*	Y			*							Y		Y							*	*	*		*				*		
14	CITd	*	*	*	*	*	Y			*				Y				Y	Y						*	*	*	*	*	*				*		
15	CIT																																		Y	Y
16	CITv	*	*	*	*	*	Y			*				Y				Y	Y						*	*	*	*	*	*				*		
17	AITd	*	*	*	*	*	*			*	*			Y			Y								*	*	*	*	*	*	*	*		Y	Y	Y
18	AITv	*	*	*	*	*	Y			*	*			Y			Y					*	Y	Y	*	*	*	*	*	*	*	*				
19	STPp	*	*	*	*	*	*			*	Y					Y		*				Y	Y	Y	Y	Y	*	*	*	*	*	*			Y	Y
20	STP																																	Y		
21	STPa	*	*	*	*	*	*			*								Y	*	Y			Y	Y			*	*	*	*	*	*				Y
22	TF	*	*	Y	Y	*	Y			*	Y			Y			Y	Y	Y	Y		Y			Y		*	*		*	*	*		Y		Y
23	TH	*	*	*	*	*	Y			*				Y		Y		Y	Y	Y		Y			*	*	*	*	*	*	*	*		Y		Y
24	MSTd	*	Y	Y	Y	Y	*		Y	Y	Y		Y		*		*	*	*	Y							Y		Y	Y			Y	Y	Y	
25	MSTl	NR	Y	*	*	Y	*		NR?	Y	Y	*	*	*	*		*	*	*	Y							Y	*		Y			NR?	NR?	Y	
26	PO	Y					*			Y	*	*		*	*		*	*	*	*		*	*	*	Y	Y			Y	Y			Y	Y	?	
27	PIP	Y		Y	Y		Y			Y		*		*	*		*	*	*	*		*					Y						Y	Y		
28	LIP	*		Y	Y	Y	Y			Y	Y	*		Y	*		*	*	*				Y	*	Y	Y	Y			Y			Y	Y	Y	Y
29	VIP	*		Y						Y	Y	*		*	*		*	*	*						Y	Y	Y		Y					Y	Y	
30	MIP	*	*	*	*	*	*			*	*	*		*	*		*	*	*						*	*	Y							Y		
31	MCP	*	*	*	*	*	*			*	*	*		*	*		*	*	*						*	*	Y							Y		
32	DP	*	*	*	*	Y	Y			*	Y	*		*	*		*	*	*	*		*	*	*	Y	Y	Y	Y	Y					Y		Y
33	7a	*	*	*	*	*	*			*		*		*	*		*	Y			Y		Y	Y	Y	?	Y		Y				Y		Y	Y
34	FEF	*								?	Y					Y		Y		Y					Y	Y	Y		Y	Y			Y	Y		Y
35	46	*	*	*	*	*	*				*					Y		Y		Y		Y	Y	Y	*				S				Y	Y	Y	

Biographies

Maryam Beigzadeh is a PhD degree candidate in Amirkabir University of Technology, Tehran, Iran, from where she received her BS and MS degrees in the field of Biomedical Engineering. She has authored and/or co-authored some book chapters and several articles in Persian and in international scientific journals, in the field of Image Processing and Biomedical Engineering. She has also presented some articles in the related fields of endeavor at international conferences.

Seyyed Mohammad Reza Hashemi Golpayegani is Professor at the Biomedical Engineering Department of Amirkabir University of Technology, Tehran, Iran, and was Minister of Culture and Higher Education in Iran from 1983 to 1987. He has authored and co-authored numerous papers in Electrical and Biomedical Engineering, and has also been active in the field of Philosophy of Science and Engineering Education. He is credited with the publication of a number of articles in international scientific journals in the fields mentioned